Submitted to *Remote Sens.*. Pages 1 - 17.

OPEN ACCESS

Article

Using Hyperspectral Ocean Color Sensors for Monitoring Cyanobacterial Blooms in Lakes and Reservoirs.

Nicholas B. Tufillaro[1,*], Connie S. Bozarth[2], Jonathan W. Shepardson[2], Jennifer L. Graham[3], Theo W. Dreher[2,4], and Curtiss O. Davis[1]

[1] College of Earth, Ocean, and Atmospheric Science, Oregon State University, 104 CEOAS Administration Building, Corvallis, OR 97331-5503

[2] Department of Microbiology, Oregon State University, 220 Nash Hall, Corvallis, OR 97331

[3] US Geological Survey, Kansas Water Science Center, 4821 Quail Crest Place, Lawrence, KS

[4] Center for Genome Research and Biocomputing, Oregon State University.

* Author to whom correspondence should be addressed; nbt@coas.oregonstate.edu,
Tel. 541-737-3504, Fax. 541-737-2064

Version October 15, 2013 submitted to RemoteSensing. *Typeset by LaTeX using class file mdpi.cls*

Abstract: A method is illustrated for quantifying algal bloom concentrations, in particular fresh water cyanobacteria, with hyperspectral data. The method uses the hyperspectral data and spectral shape matching to the absorption features for chlorophyll and phycocyanin. The method is first developed for algal blooms in Dexter Reservoir, east of Eugene, Oregon, where hyperspectral imagery from HICO (93m) during 2012-2013, and full resolution (300m) multispectral imagery from MERIS during 2011, are used to monitor microbiologic dynamics. MERIS images provide sufficient resolution to track bloom temporal dynamics, and HICO images provide additional spectral and spatial details to address specific water quality issues, such as the presence and location of cynanobacterial blooms in the reservoir. HICO data is calibrated using *in situ* data, and a method is developed to quantify algal blooms, and in particular cyanobacterial blooms, with hyperspectral data. Initial results from two other sites, Cheney Reservoir in Kansas, and Lake Houston in Texas, are also presented. These examples demonstrate the unique capabilities of optical hyperspectral sensors for monitoring algal booms in lakes and reservoirs.

Keywords: hyperspectral; fresh water; monitoring

---

1. Introduction

Ocean color remote sensing satellites can provide valuable information about the quality of fresh water lakes and reservoirs. The detailed spectral information provided by hyperspectral sensors provide a finer look at color agents and pigments, such as those produced in Cyanobacterial Harmful Algal Blooms (CHABs). However, the potential and limits (spatially and spectrally) of current and future sensors is still being evaluated. To gauge their potential, we are using information from the Hyperspectral Imager of the Coastal Ocean (HICO) to assess water quality at a few example sites near cities and towns which are subject to regular algal blooms [1].

Recent work in fresh water remote sensing has often focused on the detection of chlorophyll concentration and algal blooms using multispectral sensors. For instance, Binding *et. al.* demonstrated the use of the MERIS Maximum Chlorophyll Index (MCI) for monitoring the Lake of the Woods [2]. Another recent study by El-Alem *et. al.* found good correlations between *in situ* chlorophyll-a concentrations and satellite imagery from lakes in the Southern Province of Quebec, Canada. [3] Algorithms for detecting cyanobacteria, often with multispectral sensors, are described in a number of recent publications [4–13]. A comprehensive overview and evaluation of the potential of remote sensing for monitoring fresh water sources is provided by Dekker and Hestir in a report by the Australia's national science agency [14]. US national agencies such as NOAA, NASA, and the EPA are also active in studying the use of remote sensing for fresh water sources [15][16]. However, to date the complexity and diversity of fresh water sources has stymied the implementation of 'operational' fresh water remote sensing products, such as those provided by NASA and NOAA for open ocean waters [17].

In this paper we illustrate a method that uses hyperspectral optical remote sensing data to detect pigments such as Chlorophyll-a and Phycocyanin. We believe hyperspectral data can aid in untangling confounding variables, such as sediments and additional color agents, in attempts to use remote sensing to evaluate fresh water quality. The hyperspectal method described in this paper starts by first estimating the Intrinsic Optical Properties (IOPs) using an extension of the Quasi-Analytical Algorithm (QAA) for fresh water bodies laden with cyanobacteria recently described by Mishira et. al., who also provide a nice overview of previous (mainly multispectral) retrieval methods for correlating cyanobacterial concentrations to optical remote sensing data [18]. We then use the estimated hyperspectral absorption spectra to identify absorption peaks using a Gaussian fitting procedure typical of laboratory assays. Unlike multispectral methods, hyperspectral data can precisely estimate the absorption maxima of a target pigment.

Our study is initially focused on Dexter Reservoir near Eugene, Oregon, which regularly has cyanobacterial blooms in the summer. The booms are a major concern because they are commonly associated with toxins and unpleasant taste-and-oder compounds, which are not associated with other phytoplankton. This study demonstrates the use of hyperspectral remote sensing to detect phycocyanin, a specific marker indicative of cyanobacteria, in Dexter Reservoir, and a few other lakes (Cheney Reservoir near Wichita, Kansas, and Lake Houston near Houston, Texas) to demonstrate general applicability.

2. Multispectral Detection of Algal Blooms in Dexter Reservoir.

Figure 1. USGS map of Dexter Reservoir southeast of Eugene, Oregon. Sites for water sampling are labeled 1 through 6.

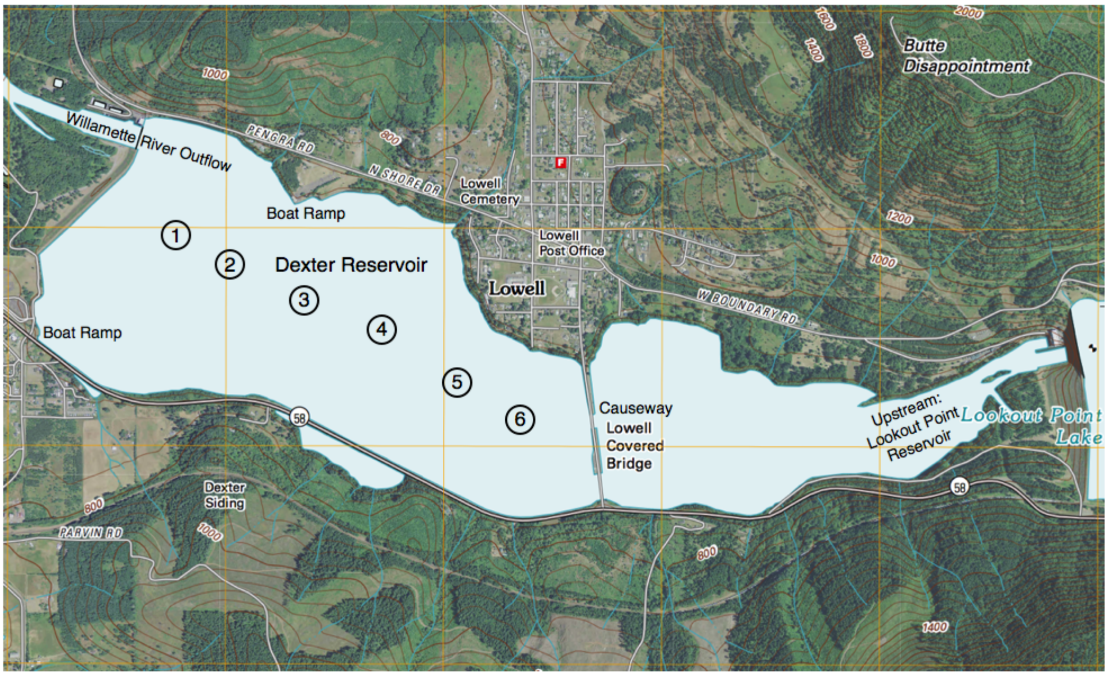

Dexter Reservoir (see Fig. 1) is a small, shallow lake about about 26 km southeast of Eugene, Oregon (43.916 N, -122.796 W) [19]. Dexter Reservoir was created in 1954 by a US Army Corps of Engineers dam and provides both flood control and recreation to the residents of Lane County, Oregon. Its aspect ratio is about 4:1, stretching in a southeast direction with a width of about 1 km. Despite being relatively shallow, thermal stratification is common in Dexter. The reservoir is fed by cool water discharge from Lookout Point Reservoir to the southeast, and these cooler waters tend to sink along a bathymetric gradient reaching a depth of about 20 meters at the northwest corner. Dexter Reservoir often exhibits algal blooms in the summer and fall, consisting of diatoms and cyanophytes, and in recent years has been subject to CHAB alerts issued by the Oregon's Health Authority (OHA) for potential toxicity [20].

We began using remote sensing to examine algal blooms in Dexter in 2011, with *in situ* sampling added in 2012. The main concern behind such monitoring is recreational and drinking water exposure to cyanotoxins such as microcystins, anatoxin, cylindrospermospin, and saxitoxin. Starting the 19th of August 2011 until 14 October 2011 (56 days), the OHA issued a CHAB warning for Dexter Reservoir. The initial warning was based cyanobacterial cell counts $>$ 100,000 cells/mL in a sample, at which time a blue green bloom was visible over extensive sections of Dexter's surface waters.

In 2011 we obtained Full Resolution (FR) — 300 meter — MERIS imagery from the Canadian Space Agency (CSA) in near real-time. MERIS was the European Space Agency's (ESA) primary ocean color sensor [21]. We used MERIS to monitor Dexter Reservoir from 2011 until March of 2012 (when MERIS ceased operation). Dexter Reservoir's small size provides a test of the spatial limits of detection with

MERIS. Dexter Reservoir is approximately 4 x 1 km in size resulting in 1 to 3 MERIS pixels imaging the reservoir; as expected the small size causes adjacency effects from land which compromises our ability to distinguish signals originating from the water body. Nevertheless, as the results below demonstrate, the spatial sampling of FR MERIS is sufficient to detect algal blooms in Dexter Reservoir.

We computed the Maximum Chlorophyll Index (MCI) from both Level 1 and Level 2 FR MERIS data subsetted around Dexter Reservoir. MCI is a 'Line Height' algorithm originally introduced by Gower *et al.* [22] to detect ocean surface algal booms, and also recently used by Binding *et al.* for detection of algal blooms in lakes [2]. The MCI index for MERIS was computed using bands (8,9,10) with wavelengths centered at (681, 705, 753) nm. Figure 2 shows Dexter Reservoir as seen by FR MERIS along with a map of the MCI index using Level 2 data processed with ESA's BEAM L2 processor. A MCI map for Dexter is shown for 2 August 2011 and 27 August 2011, dates before and during the CHAB warning from the OHA. The MCI index clearly shows the change in the water quality, as well as giving a rough indicator for the distribution of phytoplankton, suggesting the highest concentration in the southern section of the reservoir. Figure 2 demonstrates that the MERIS MCI index can be used to monitor algal blooms in Dexter Reservoir, despite this detectors spatial resolution.

Figure 2. Use of the Maximum Chlorophyll Index (MCI) to detect a cyanobacterial bloom in Dexter Reservoir during August 2011. The RGB image shows little difference before (a) and during (b) an algal bloom. The MCI maps (c,d), though, clearly indicates the presence of a algal bloom on 27 of August as indicated by the green, yellow, and red pixels.

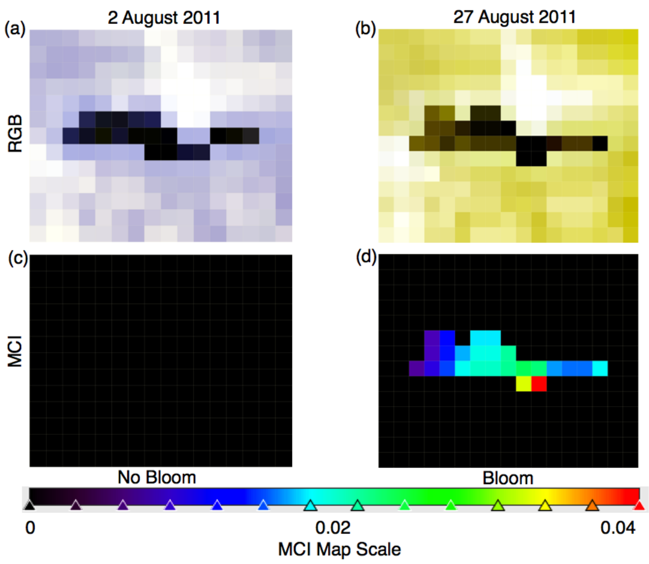

A time series of the MCI Index is shown in Figure 3 computed by taking the largest MCI value within Dexter Reservoir each day data was available. The horizontal axis indicates days from 1 August 2011, and shows a detectable MCI index on 15 August 2011. The 'peak' of the bloom, as indicated by Figure 3, occurred on the 27th August 2011, and the bloom appears to be diminishing by 11 September 2011. Note that, while the boom onset was accurately reflected in the start of the OHA posting period, this was not true of its decline, since continuous official monitoring was not conducted and the 14th October 2011 date for lifting the posting was well after visible clearance of the bloom had occurred.

A MERIS overpass of Dexter Reservoir occurs about once every other day, and during the 54 day period shown in Fig. 3 there were MERIS overpasses on 28 days, 13 days of which were cloudy, leaving 15 days when we were able to retrieve clear images of Dexter Reservoir. In 2011 we did not have *in situ* chlorophyll concentration data to correlate with MERIS data, but the result shows that with relatively simple processing, a sensor with the spatial and spectral resolution of FR MERIS can be used to monitor significant changes in algal bloom activity in Dexter Reservoir despite its small size.

Figure 3. A daily time series from Dexter Reservoir showing changes in the intensity of an bloom as indicated by the Maximum Chlorophyll Index (MCI) during August-September 2011.

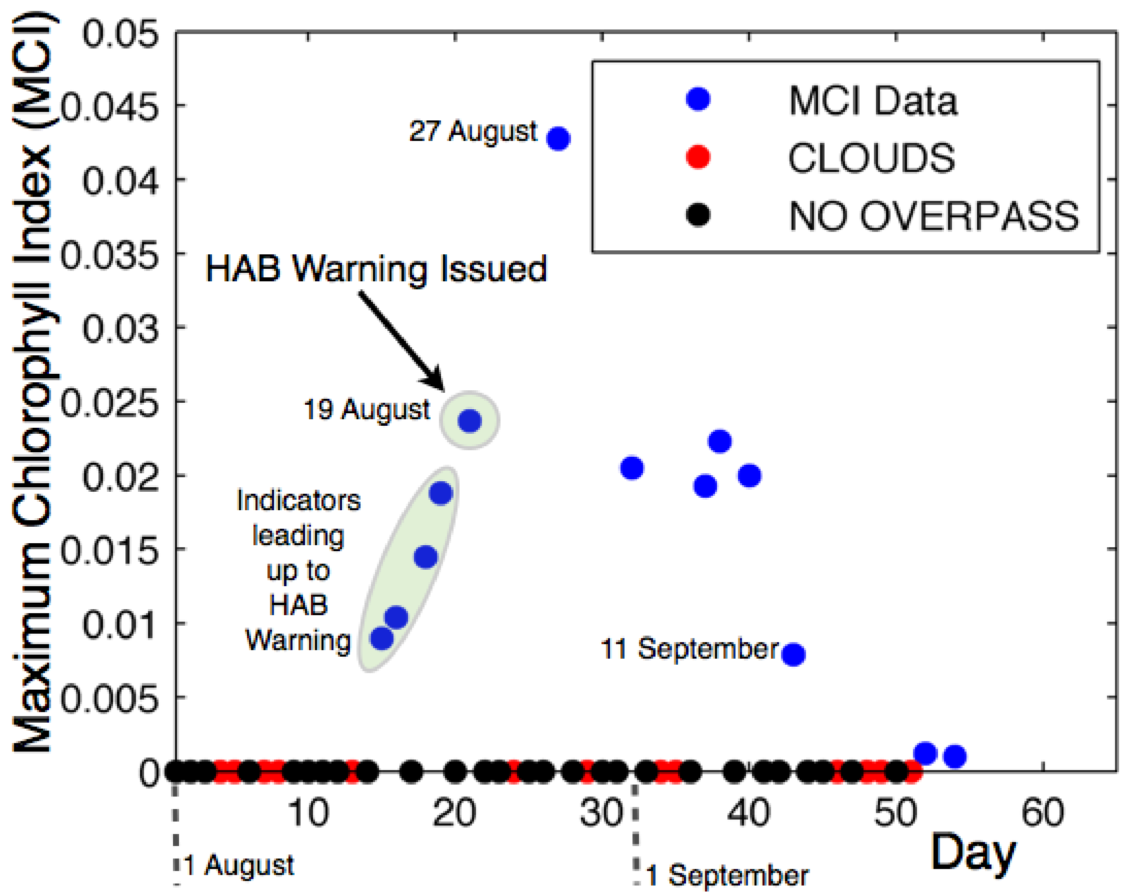

3. Hyperspectral Monitoring of Dexter Reservoir During 2012-2013

Based on the initial results in 2011, during 2012-2013 and we took a more detailed look at Dexter Reservoir by using water sampling and hyperspectral remote sensing using HICO which operates on the International Space Station (ISS) [1,23]. HICO is an imaging spectrometer with a spatial coverage (swath size) of 50 by 200 km, a spatial resolution of ≈ 100 meters, and spectral coverage from 400 to 900 nm with a 5.7 nm spectral sampling. Request for images from HICO for specific sites are made from HICO's academic web portal at Oregon State University [24]. HICO is a demonstrator limited to taking one scene per orbit and sampling is further constrained by the ISS orbit and scheduling priorities.

Table 1. Table of HICO observation schedule of Dexter Reservoir acquired in 2012-2013. Pacific Standard Time (PDT) is 7 hours behind UTC.

Date (UTC)	Angle (from Nadir)	Status	CHAB Warning
2012-06-26 21:33:21	-38.2	Cloudy	No
2012-06-28 21:21:58	10.7	Cloudy	No
2012-07-10 21:51:16	1	Clear	No
2012-07-11 16:06:35	-2.8	Clear	No
2012-07-13 20:45:28	-6.3	Clear	No
2012-07-23 16:41:20	6.8	Clear	No
2012-07-26 15:39:37	-5.7	Cloudy	No
2012-08-22 23:08:03	-13.4	Clear	Yes
2012-09-02 19:04:33	6.3	Clear	Yes
2012-09-04 23:55:43	-30.1	Clear	Yes
2012-09-20 17:25:05	-8.3	Cloudy	Yes
2013-03-02 18:59:23	-18.7	Cloudy	No
2013-05-07 17:08:21	8.8	Clear	No
2013-06-29 18:59:23	-30.5	Clear	No
2013-07-02 00:27:15	7.6	Clear	No
2013-07-08 21:58:27	-14.3	Clear	Yes
2013-07-10 15:20:10	-17.8	Clear	Yes
2013-07-24 15:32:10	3.5	Cloudy	Yes
2013-09-03 23.12.28	0.5	Cloudy	Yes

Because of its limited sampling, data from HICO is not useful for continuous temporal monitoring of algal bloom dynamics in Dexter Reservoir, but we were able to use HICO's detailed spectral and spatial coverage to derive information both about pigment functional groups, specifically phycocyanin, and their spatial coverage. Data from HICO was scheduled and collected on the dates and times shown in Table 1.

Clear images of Dexter Reservoir were obtained on 7 days from June-September 2012, and 5 days in 2013. The best data were from 23 July, 22 August, 2 and 4 September during 2012, along with 7 May, 29 June, 1 July,8 July and 10 July during 2013. The 2012 images from 10-13 July are 'useable,' but low lying cloud or haze (possibly smoke) obscures the view. The 23 July date was relatively clear of bloom, while on the 22 August, 2 and 4 September dates HICO shows significant phytoplankton concentrations. In 2013, the 8 and 10 July images show a bloom, while the earlier dates are bloom free. We obtained same day *in* situ data from water samples which we use to correlated with the remote sensing data on 4 September 2012, and 29 June and 8 July, 2013.

A CHAB warning for Dexter Reservoir was issued by Oregon Health Authority (OHA) from 31 July through 16 November 2012, and 3 July through 19 September during 2013. In addition, water samples were collected with a boat from six sites located by GPS along a transect running down the center of the reservoir on 6/26, 7/11, 7/23, and 9/4 in 2012, and 6/29, 7/8, 7/20, and 7/23 during 2013. An integrated water column sampler (1.5 cm i.d.) was used to collect water at a depth equal to twice the Secchi depth, or to the lake bottom, which ever was shallower. Water from the sample was mixed in a bucket and then a subsample of 250 ml was collected for transport to the lab where 50 ml was filtered for chlorophyll analysis, and 100 ml was filtered for phycocyanin analysis. Correlations between *in situ* samples and remote sensing data for 4 September 2012, and 29 June, 8 July 2013 are used in this paper. Phycocyanin concentrations for the six sites where water samples where collected are shown in Fig. 4.

Figure 4. Phycocyanin concentrations from *in situ* sampling for (a) 2012 and (b) 2013. Digital Latitude (N) - Longitude (W) for sites 1-6 (see Fig. 1): (43.919, -122.803), (43.918, -122.800), (43.916, -122.796), (43.915, -122.792), (43.913, -122.787), (43.912, -122.783).

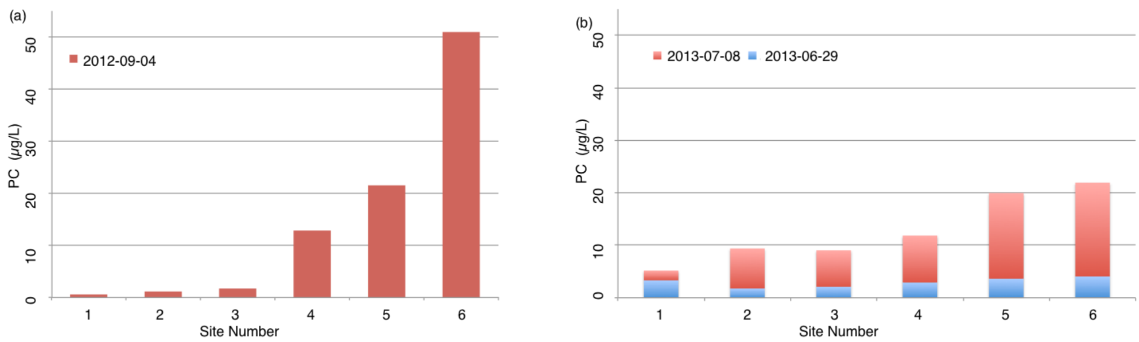

The remote sensing spectral data were atmospherically corrected with the Tafkaa 6s code to compute Level 2 above water remote sensing reflectance (L2, R_rs) for HICO [25,26]. The L2 images are further subsetted and geolocated using ground control points around Dexter Reservoir. The results are shown in Figure 5 from before and during a cyanobacterial bloom in August 2012. The reflectance is nearly 2.5 times brighter during the algal bloom.

Figure 5. Images of Dexter Reservoir using imagery from HICO. The reservoir looks relatively clear on (a) 23 July 2012, but on (b) 22 August 2012, Dexter Reservoir looks very bright, indicating an algal bloom. The approximate spatial resolution (pixel size) of HICO is 100 meters. These RGB images were created with the spectral bands: (700, 560, 450) nm to enhance the view of chlorophyll in the water.

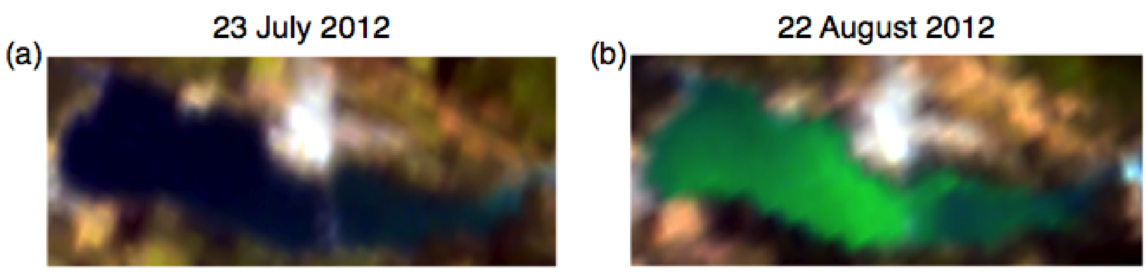

Spectra from 2 September 2012 are shown in Figure 6 to discuss salient features. In physically and biologically active inland waters, the water leaving radiance can result from a rich mixture of absorption and scattering processes. However, the spectra from the bloom examples from Dexter roughly can be understood by considering the major absorption processes during the bloom. If we assume that the spectral shape of reflected light to a first approximation is determined by the major absorption processes, then the reflected peaks seen at approximately 550 nm and 700 nm correspond to minimums for absorption by phytoplankton pigments. Fluorescence from phycocyanin around 650 nm and chl-a near 680 nm also contribute to the observed reflectance spectra (Figure 6).

Figure 6. Examples of remote sensing reflectance spectrum from Dexter Reservoir highlighting the absorption processes determining the basic shape of the spectrum during an cyanobacterial bloom. Each curve corresponds to a different location in the reservoir (see inset).

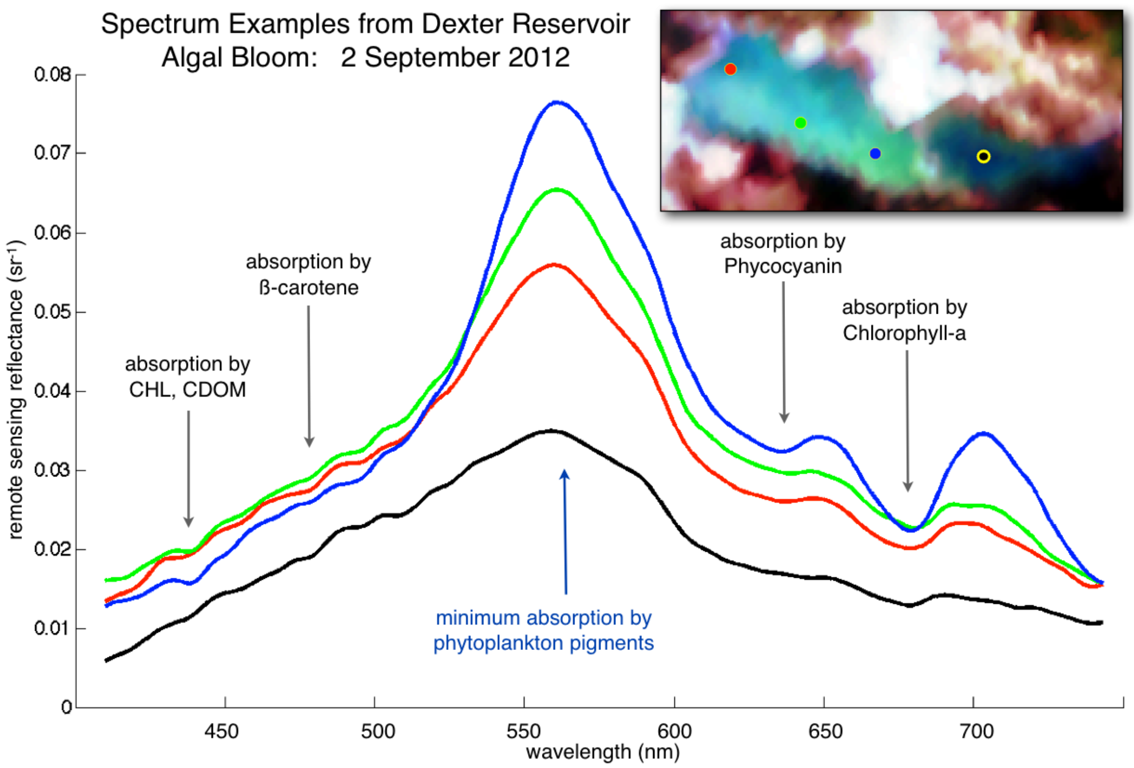

4. Method For Estimating Absorption Peaks from Hyperspectral Images.

To make these observations about absorption quantitative, we computed the intrinsic optical properties (IOP's) using the Quasi-Analytical Algorithm (QAA) [27], recently modified for lakes by Mishra et. al. [18,28]. The algorithm starts with the L2 remote sensing reflectance and estimates the total backscattering coefficient and absorption coefficient for each water image pixel. The IOP absorption, is then used to identify and estimate the amplitudes of absorption peaks associated with specific pigments, in particular chlorophyll-a which is correlated to total phytoplankton concentrations, and phycocyanin which can be correlated to cyanobacteria.

The absorption and scattering along a transect across the center of Dexter Reservoir is shown in the inset of Figure 7. The increase in the backscattering coefficient approaching the southeast corner of the reservoir explains the increase in brightness. The absorption peaks for both chlorophyll-a and phycocyanin are also easily identified. To estimate the relative amounts of chlorophyll-a and phycocyanin we modeled the absorbance spectra between 600 and 700 nm with two Gaussian functions and estimated all the parameters in the two Gaussians, the means (μ), standard deviations (σ), and amplitudes (A), using a Nelder-Mead optimization [29]. In this method we first estimate the linear background, or so-called 'continuum' signal, before the peak finding [30]. Thus the method is like a line-height method except that it uses all the available hyperspectral data to estimate the location and amplitude of the absorbance. Since it is a nonlinear optimization, the method can find multiple solutions (local minima), however for the data shown here the method returned a unique and consistent solution for each spectrum along the transect. Figure 8 shows a typical fit of how the two Gaussians approximate the absorbance spectrum.

Figure 7. (a) Absorbance and (b) scattering calculated using QAA along (c) a transect along a middle section of Dexter reservoir for 4 September 2012. The color indicating the site location changes from blue to red from the northwest to the southeast corners

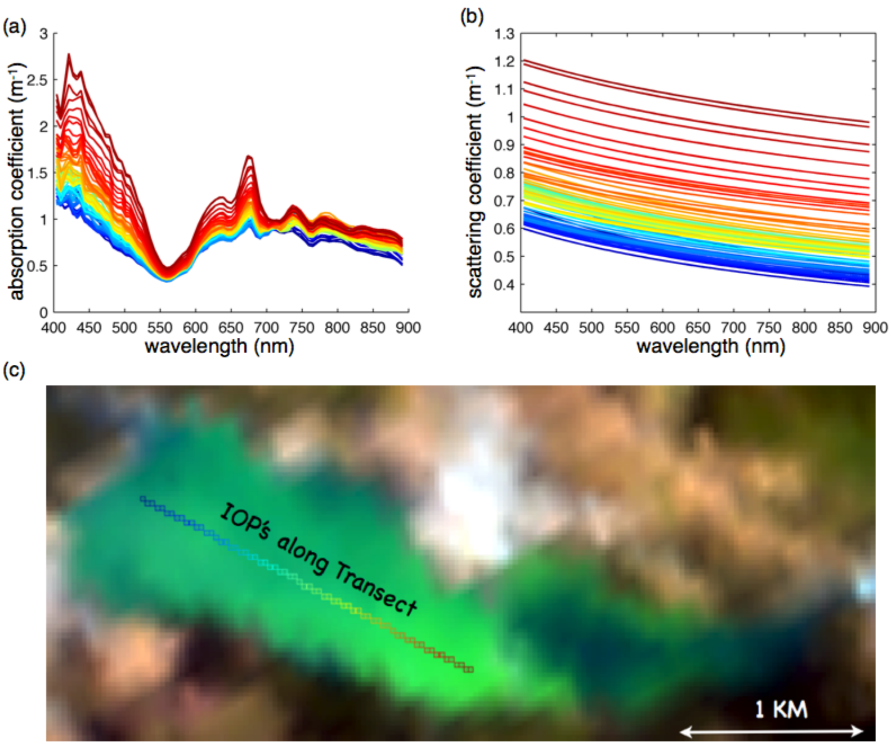

As shown in Figure 9 the method finds a consistent center (mean) for both Gaussians across the transect. For 2 September 2012 the mean maximma (with standard deviation) are 625.5 $\pm$ 1.5 nm and 673.4 $\pm$ 1.2 nm. The estimate for the amplitude of each Gaussian is also shown in Fig. 9. Similar results are also presented for 4 September 2012, with Gaussian fits yielding maxima of 628.4 $\pm$ 1 nm and 672.0 $\pm$ 1.3 nm.

Coincident data from HICO and water samples are shown in Fig. 10, the plots show an empirical correlation between the Gaussian amplitudes and the *in situ* measurements of phycocyanin and chlorophyll-a concentrations at six sites on three different days. As mentioned, the Gaussian fits are made from the estimated absorption spectra computed from the hyperspectral remote sensing data. The

Figure 8. Peak Finding (using nonlinear optimization for fitting Gaussians) locates two peaks with nearly the same centers in absorbance along the whole transect which are proportional to Phycocyanin and Chlorophyll-a concentrations.

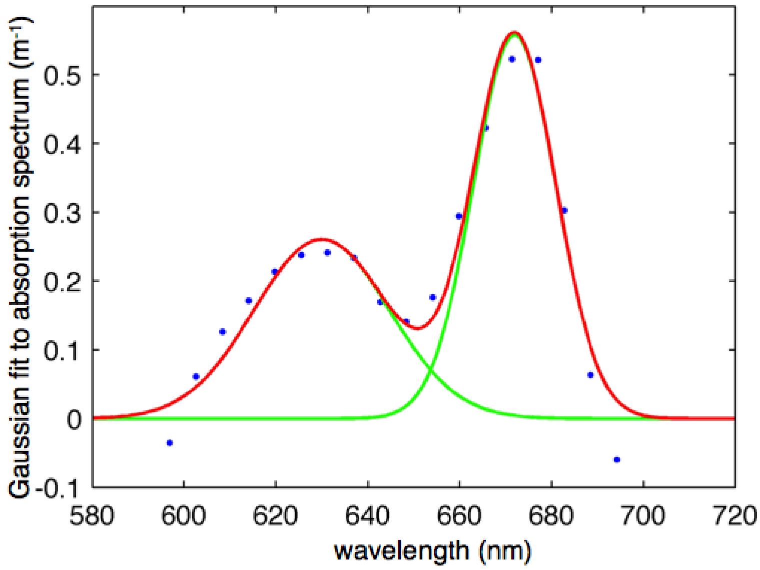

samples from 4 September 2012 (green) and 8 July 2013 (red) are from dates during a bloom, and have high phycocyanin values relative to 29 June 2013 (green) which immediately preceded the 2013 bloom. The data from 2012 (red) are also systematically higher than the 2013 samples, this may be an artifact of the algorithm which subtracts the continuum signal (a linear base line) from the spectra before estimating the Gaussian amplitudes. A linear estimate for the trend for Chlorophyll-a (Fig. 10(a)) is $y_{chl} = 0.0025 \cdot x + 0.1$ with an $R^2 = 0.83$, and for Phycocyanin (Fig. 10(b)) $y_{ph} = 0.013 \cdot x + 0.06$ with an $R^2 = 0.69$.

It is useful to also track the ratio of Phycocyanin to Chlorophyll-a. For the *in situ* samples the ratio varies from about 1:2 to 6:1, with higher ratio values typically occurring with more intense blooms. We also attempted to estimate the Phycocyanin to Chlorophyl-a ratio from remote sensing data. A simple ratio of Gaussian line height (i.e., the amplitude of the Gaussian fits at $\approx$ 630 nm to and $\approx$ 675 nm) does not lead to a significant correlation. To improve the correlation, we assume that the absorbance is proportional to $\epsilon \cdot C$, where ϵ is the 'efficiency' and C is the 'concentration' of the pigment. The efficiency is not necessarily the quantum efficiency, but rather an overall constant relating the change in the Gaussian line height to the change in pigment concentration. This 'empirical efficiency' factor is the slope in the linear regression for the plots shown in Fig. 10, thus $\epsilon_{ph} = 0.013$ and $\epsilon_{chl} = 0.0025$, or $\approx$ 5:1. Correcting the Gaussian line heights between Phycocyanin and Chlorophyll-a for this efficiency ratio results in the correlation shown in Fig. 11. The correspondence between the *in situ* and the from remote sensing ratio is essentially one-to-one after the correction, with $y_{ph/chl} = 0.99 \cdot x + 0.17$ with $R^2 = 0.88$. Note that the correction — and hence the remote estimation of the ratio of concentrations — requires the use of *in-situ* data for calibration.

5. Additional Examples of Absorption Spectra

Figure 9. The Gaussian fits for absorption by Chlorophyll-a (blue) and Phycocyanin (red). The top row is data for a transect down the center of the reservoir from 2 September 2012 (a) center of Gaussians (means), (b) amplitudes of Gaussians. Data from 4 September 2012 (c) center of Gaussians (means), and (d) amplitudes of Gaussians. The site numbers run down the middle section as indicated in Fig. 7(c).

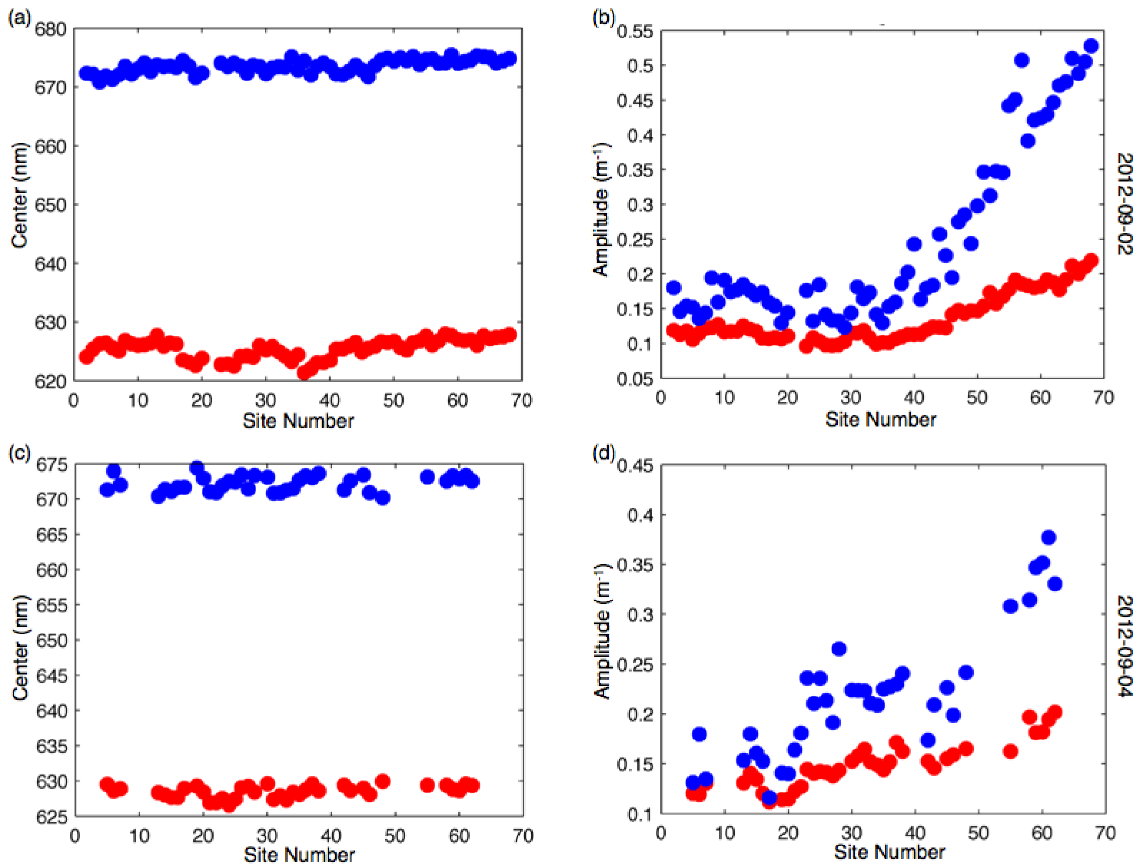

We tested our method at two other sites, Cheney Reservoir in Kansas, and Lake Houston in Texas. Cheney Reservoir supplies the city of Wichita, KS, and has experienced taste and odor problems in its water for several years related to summer algae blooms. Additionally, Cheney has significant suspended sediments and high phosphorus levels from agricultural and livestock activities. Lake Houston supplies Houston, TX. Algal blooms often cause hypoxia in Lake Houston, which is normally well stocked bass and other sport fish.

Coincident HICO images and water samples were obtained for Cheney Reservoir and Lake Houston in 2013 for the dates and times shown in Table 2.

A summary results of the Cheney sampling are presented in Fig. 12. The Chlorophyll concentration varies from a high of approximately 30 $\mu g/L$ to 6 $\mu g/L$; while Phycocyanin varies from 15 $\mu g/L$ to 2 $\mu g/L$. A linear regression on the remote sensing and *in situ* data is shown in Fig. 12 (c)-(d) with $y_{chl} = 0.0064 \cdot x - 0.0076$ with an $R^2 = 0.93$, and for Phycocyanin $y_{ph} = 0.0034 \cdot x + 0.025$ with an $R^2 = 0.82$. The ratio of slopes is PC:CHL $\approx$ 1:2.

A summary results of the Lake Houston sampling are presented in Fig. 13. Six water samples where collected at the sites labeled 1-6 in Fig. 13(a). Low lying scattered clouds and a thick haze obscured the view of the Lake. A land mask (Fig. 13(b)) provides a better view of the lake, though it is overly

Figure 10. Correlation between *in situ* (a) chlorophyll-a and (b) phycocyanin concentrations, and their respective amplitudes from Gaussian Fits at ≈ 675 nm and ≈ 630 nm across a transect down the center of Dexter Reservoir. The red dots are data from 4 September 2012, green dots are 29 June 2013, and the blue dots are 8 July 2013. The lower values of Phycocyanin during 29 June 2013 ((b) green dots) indicate that this day is CHAB free relative to the the other two dates.

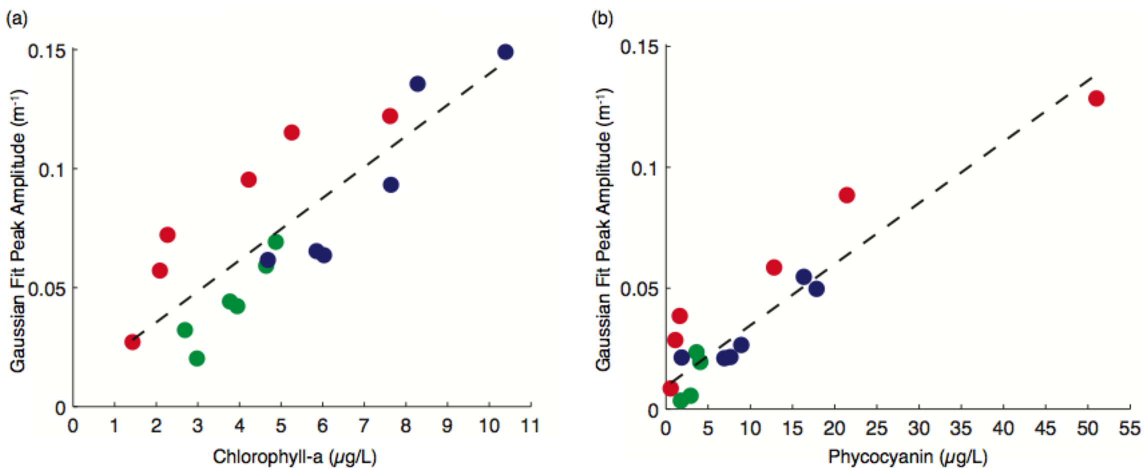

Table 2. Table of Co-incident HICO observations and *i*n situ collections for additional reservoirs. Both sites are Central Daylight Time (CDT), 5 hours behind UTC.

Site	HICO Date (UTC)	Angle from Nadir	Conditions
Cheney Reservoir	2013-06-22 20:30:51	22.4	Clear Sky, High Suspended Sediment
Lake Houston	2013-07-25 14:50:42	-1.1	Heavy Haze

aggressive, masking out a number of water sections as well. Despite the difficult conditions, we where still able to get remote sensing retrievals for all the sites except for site 1 (very heavy haze) since the concentrations are high for both Chlorophyll (≈ 35-95 $\mu g/L$) and Phycocyanin (≈ 15-45 $\mu g/L$), resulting in good fits for the Gaussian Line Heights as shown in Fig. 13(c) from site 6 (orange dot), which had the lowest pigment concentrations. A linear regression on the remote sensing and *in situ* data is shown in Fig. 12 (d)-(e) for both Chlorophyll-a $y_{chl} = 0.0018 \cdot x + 0.092$ with an $R^2 = 0.60$, and Phycocyanin $y_{ph} = 0.0020 \cdot x + 0.041$ with an $R^2 = 0.62$. The ratio of slopes is PC:CHL ≈ 1:1.

At all sites it appears the Gaussian fit retrieval method (because it utilizes a narrow bandwidth available from the hyperspectral data) is able to estimate useful line height values despite complications due to sediments and haze.

6. Discussion and Conclusions

We made use of a recently introduced QAA algorithm for fresh water cyanobacterial blooms, adapting it for use with HICO data, and adding a peak finding algorithm, which allows us to use the hyperspectral capabilities of HICO to identify and correlate the absorption of phycocyanin and chlorophyll-a with *in situ* sampling. These results show the potential of hyperspectral imagers to routinely map specific

Figure 11. Correlation between the ratio of *in situ* Phycocyanin to Chlorophyll-a concentrations and the remote sensing Gaussian Line Heights after an 'empirical efficiency' correction. The one-to-one correlation shows that, after *in situ* calibration and correction, remote sensing data can be used to estimate the ratio of Phycocyanin to Chlorophyll-a concentrations.

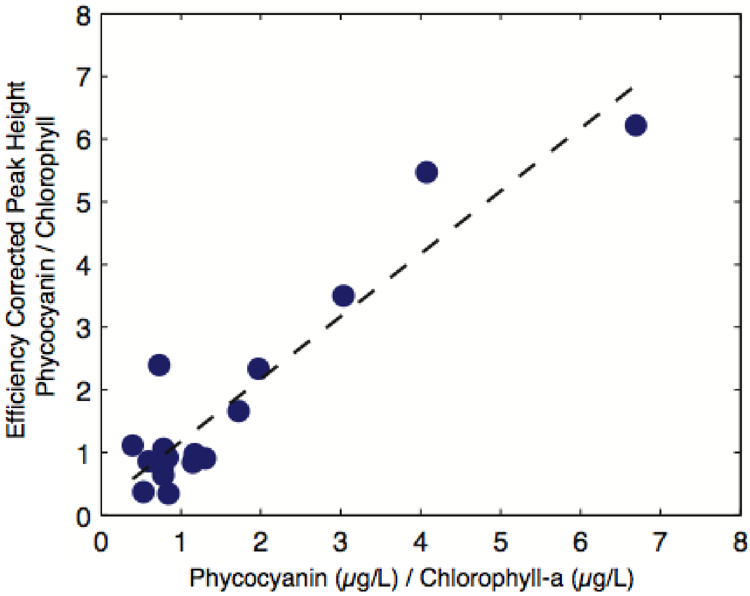

pigments in lakes. Algorithms for data from multispectral sensors, such as MCI, are useful for identifying the presence of an algal bloom, but they do not have the spectral resolution to identify specific pigments, such as phycocyanin associated with specific functional groups of phytoplankton. Additional examples of peak finding for chlorophyll-a and phycocyanin using HICO hyperspectral data are also illustrated in a range of lakes, one with high sediment, and another with a thick haze. Future sensors like NASA's proposed HyspIRI (60m, hyperspectral) [31] could use this method for hyperspectral monitoring of water quality in lakes and reservoirs. With additional validation, the methods described in this paper could be made operational, thereby providing automated and routine information for water quality managers using data from HyspIRI or similar sensors.

Additionally, we examined cyanobacterial blooms in Dexter Reservoir southeast of Eugene, OR, using full resolution (FR 300 meter) multispectral MERIS imagery, which provides a comparison to hyperspectral images at 100 meters resolution from HICO. The examples in this paper also illustrate the potential of high resolution sensors such as ESA's Sentinel-3 Ocean and Land Color Instruments (OLCI) for monitoring algal blooms in smaller lakes and reservoirs.

This study also shows that sensors with higher spatial resolution, such as HICO, can provide valuable information on the spatial variation of bloom even for smaller reservoirs, which can be used guide selection of optimal sampling sites, or to track overall bloom dynamics.

Acknowledgements

We thank Jasmine Nahorniak for providing detailed comments on a early version of this manuscript and Zhongping Lee and Sachi Mishra for discussions about the QAA algorithm.

Figure 12. Cheney Reservoir, KS, 22 June 2013: (a) HICO image 3:30 PM CDT, six water samples where taken from the center of the Reservoir at the locations indicated by dots (dark blue, North to orange, South); (b) A land masked was applied to a pseudo-color RGB image (700 nm, 560 nm, 451 nm) to emphasize variations in water color; (c) Regression between remote-sensing Gaussian fit Line Height and *i*n situ Chlorophyll-a measurements; (d) Regression between remote-sensing Gaussian fit Line Height and *i*n situ Phycocyanin measurements.

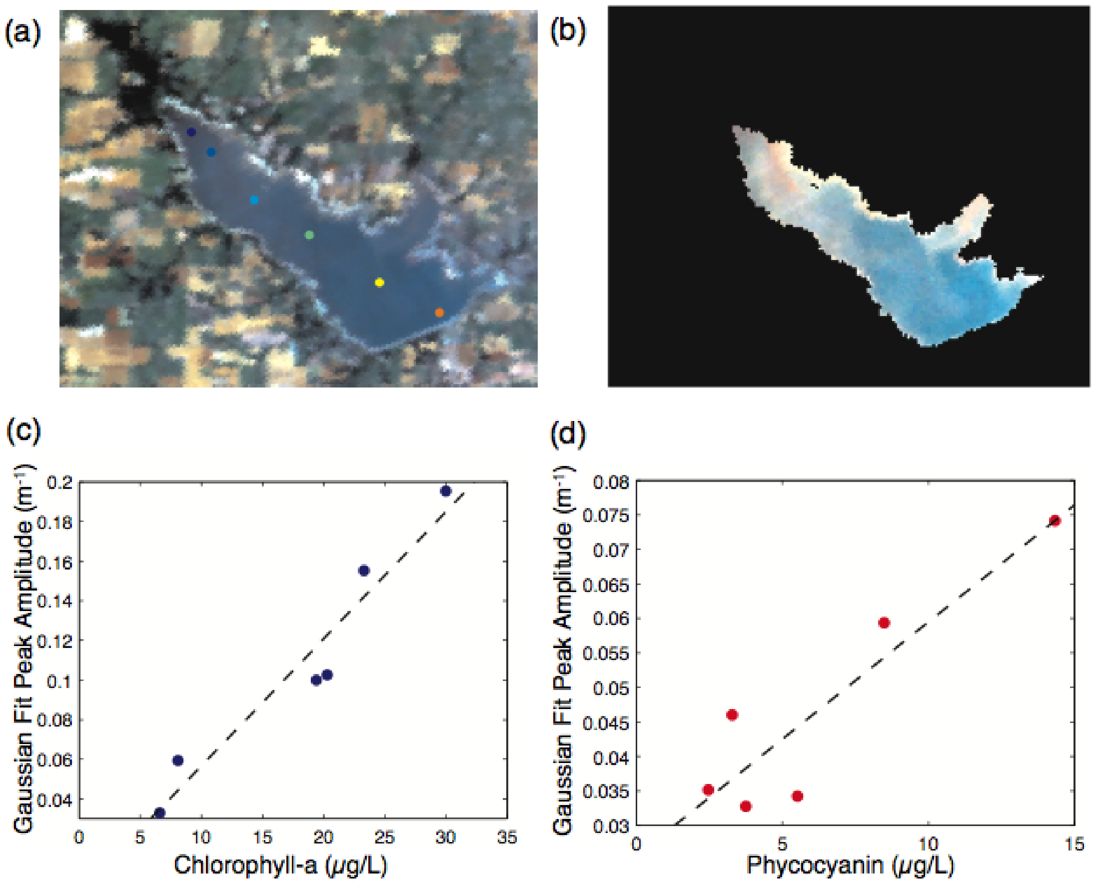

References

1. Corson, M.R.; Davis, C.O. A New view of Coastal Oceans From the Space Station. *EOS Trans. AGU* **2011**, p. 161.
2. Binding, C.E.; Greenberg, T.A.; Bukata, R.P. Time series analysis of algal blooms in Lake of the Woods using the MERIS maximum chlorophyll index. *Journal of Plankton Research* **2011**, *33*, 1847–1852.
3. El-Alem, A.; Chokmani, K.; Laurion, I.; El-Adlouni, S. Comparative Analysis of Four Models to Estimate Chlorophyll-a Concentration in Case-2 Waters Using MODerate Resolution Imaging Spectroradiometer (MODIS) Imagery. *Remote Sensing* **2012**, *4*, 2373–2400.
4. Hunter, P.; Tyler, A.; Willby, N.; Gilvear, D. The spatial dynamics of vertical migration by Microcystis aeruginosa in a eutrophic shallow lake: A case study using high spatial resolution time-series airborne remote sensing. *Limnol. Oceanogr.* **2008**, *53*, 2391–2406.

Figure 13. Lake Houston, TX, 22 June 2013: (a) HICO image 9:50 AM CDT, six water samples where taken from the Lake at the locations indicated by dots (dark blue, 1 to orange, 6); (b) A land masked was applied to a pseudo-color RGB image (700 nm, 560 nm, 451 nm) to emphasize variations in water color; (c) Gaussian Fit to absorption peaks for Phycocyanin and Chlorophyll-a at site 6 (orange dot); (d) Regression between remote-sensing Gaussian fit Line Height and *in*situ Chlorophyll-a measurements; (e) Regression between remote-sensing Gaussian fit Line Height and *in*situ Phycocyanin measurements.

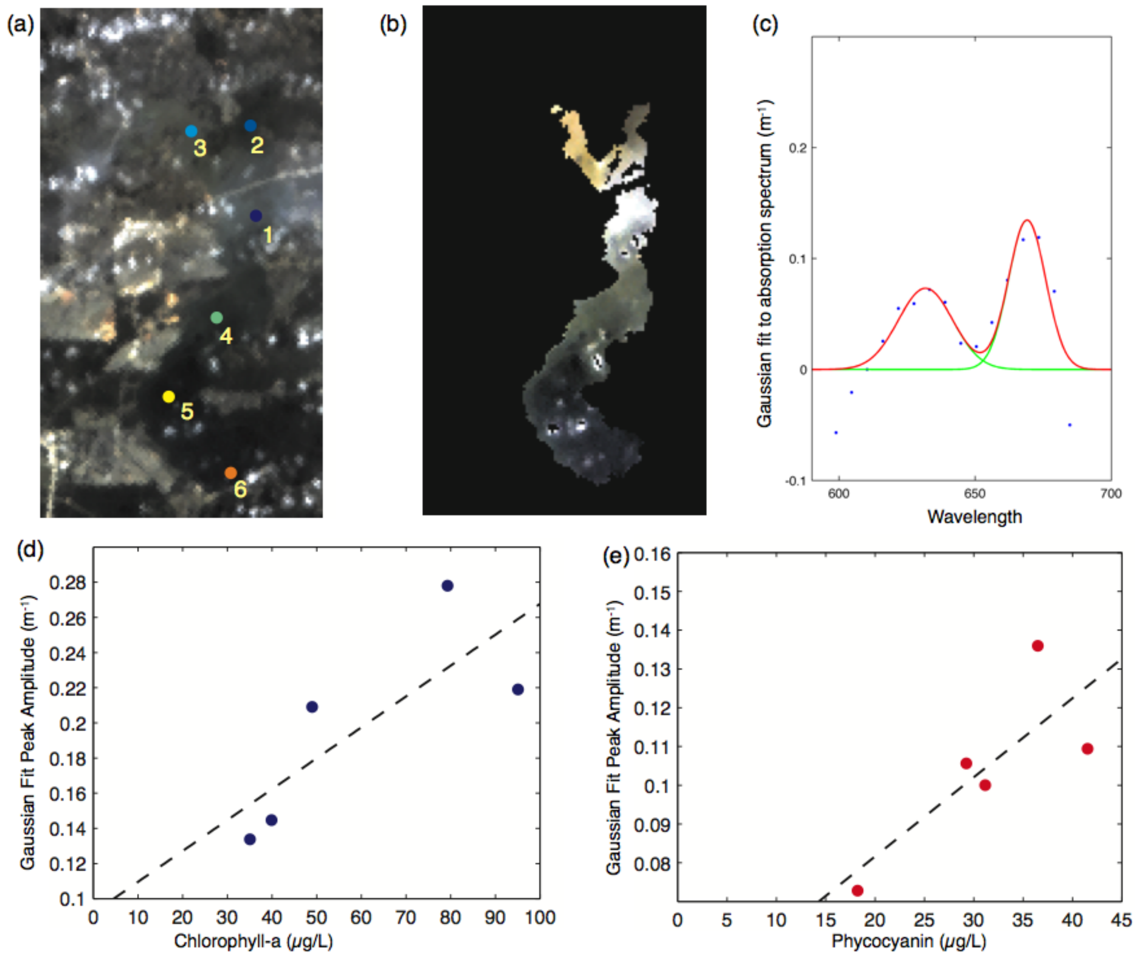

5. Hunter, P.; Tyler, A.; Gilvear, D.; Willby, N. Using Remote Sensing to Aid the Assessment of Human Health Risks from Blooms of Potentially Toxic Cyanobacteria. *Environ. Sci. Technol.* **2009**.
6. Hunter, P.; Tyler, A.; Carvalho, L.; Codd, G.; Maberly, S. Hyperspectral remote sensing of cyanobacterial pigments as indicators for cell populations and toxins in eutrophic lakes. Remote Sensing of Environment **2010**. *14*, 2705–2718.
7. Kutser, T. Passive optical remote sensing of cyanobacteria and other intense phytoplankton blooms in coastal and inland waters. *International Journal of Remote Sensing* **2009**, *30*, 4401–4425.

8. Maberly, S.; Elliott, J. Insights from long-term studies in the Windermere catchment: external stressors, internal interactions and the structure and function of lake ecosystems. *Freshwater Biology* **2012**, *57*, 233–243.
9. Matthews, M.. A current review of empirical procedures of remote sensing in inland and near-coastal transitional waters. *Intl J. Remote Sensing*, *32*, 6855–6899.
10. Ruiz-Verdu, A.; Simis, S.; de Hoyos, C.; Gons, H.; Pea-Martinez, R. An evaluation of algorithms for the remote sensing of cyanobacterial biomass. *Remote Sensing of Environment* **2008**, *112*, 3996–4008.
11. Remote sensing of the cyanobacterial pigment phycocyanin in turbid inland water. *Limnol. Oceanogr.* **2005**, *50*, 37–245.
12. Influence of phytoplankton pigment composition on remote sensing of cyanobacterial biomass. *Remote Sensing of Environment* **2007**, *106*, 414–427.
13. Mapping cyanobacterial blooms in Lake Champlain's Missisquoi Bay using QuickBird and MERIS satellite data. *J. Great Lakes Res.* **2012**, *38*, 68–75.
14. Dekker, A.; Hestir, E. Evaluating the feasibility of systematic inland water quality monitoring with satellite remote sensing. *Commonwealth Scientific and Industrial Research Organization, Canberra, Australia* **2012**.
15. Schnetzer, A.; Miller, P.; Schaffner, R.; Stauffer, B.; Jones, B.; Weisberg, S.; DiGiacomo, P.; Berelson, W.; Caron, D. Pseudo-nitzschia spp. and domoic acid in the San Pedro Channel and Los Angeles harbor areas of the Southern California Bight, 2003-2004. *Harmful Alage* **2007**, *6*, 372–387.
16. Schaeffer, B.; Hagy, J.; Conmy, R.; Lehrter, J.; Stumpf, R. An Approach to Developing Numeric Water Quality Criteria for Coastal Waters Using the SeaWiFS Satellite Data Record. *Harmful Algae* **2012**, pp. 916–922.
17. http://oceancolor.gsfc.nasa.gov/.
18. Mishra, S.; Mishra, D.R.; Lee, Z.; Tucker, C.S. Quantifying cyanobacterial phycocyanin concentration in turbid productive waters: A quasi-analytical approach. *Remote Sensing of Environment* **2013**, *133*, 141 – 151.
19. http://aol.research.pdx.edu/?q=lake/431.
20. http://www.deq.state.or.us/wq/algae/algae.htm.
21. https://earth.esa.int/web/guest/missions/esa-operational-eo-missions/envisat/instruments/meris.
22. Gower, J.; King, S.; Yan, W.; Borstad, G.; Brown, L. Use of the 709 nm band of MERIS to detect intense plankton blooms and other conditions in coastal waters. Proc. MERIS User Workshop, 2003.
23. Lucke, R.L.; Corson, M.; McGlothlin, N.R.; Butcher, S.D.; Wood, D.L.; Korwan, D.R.; Li, R.R.; Snyder, W.A.; Davis, C.O.; Chen, D.T. Hyperspectral Imager for the Coastal Ocean: instrument description and first images. *Appl. Opt.* **2011**, *50*, 1501–1516.
24. http://hico.coas.oregonstate.edu.
25. Montes, M.J.; Gao, B.C. NRL Atmospheric Correction Algorithms for Oceans: TAFKAA User's Guide. *NRL Report* **2004**, pp. 1–39.

26. Gao, B.C.; Montes, M.J.; Ahmad, Z.; Davis, C.O. Atmospheric Correction Algorithm for Hyperspectral Remote Sensing of Ocean Color from Space. *Appl. Opt.* **2000**, *39*, 887–896.
27. Lee, Z.; Carder, K.L.; Arnone, R.A. Deriving Inherent Optical Properties from Water Color: a Multiband Quasi-Analytical Algorithm for Optically Deep Waters. *Appl. Opt.* **2002**, *41*, 5755–5772.
28. Mishra, S.; Mishra, D.; Lee, Z. Bio-Optical Inversion in Highly Turbid and Cyanobacteria-Dominated Waters. *Geoscience and Remote Sensing, IEEE Transactions on* **2013**, pp. 1–14.
29. Nelder, J.A.; Mead, R. A Simplex Method for Function Minimization. *The Computer Journal* **1965**, *7*, 308–313.
30. Brown, A. Spectral curve fitting for automatic hyperspectral data analysis. *Geoscience and Remote Sensing, IEEE Transactions on* **2006**, *44*, 1601–1608.
31. http://hyspiri.jpl.nasa.gov.